# Prediction of strong ground state electron and hole wave function spatial overlap in nonpolar GaN/AlN quantum dots

S. Schulz, M. A. Caro, and E. P. O'Reilly

Citation: Appl. Phys. Lett. **101**, 113107 (2012); doi: 10.1063/1.4752108
View online: http://dx.doi.org/10.1063/1.4752108
View Table of Contents: http://aip.scitation.org/toc/apl/101/11
Published by the American Institute of Physics

# Prediction of strong ground state electron and hole wave function spatial overlap in nonpolar GaN/AlN quantum dots

S. Schulz,[1] M. A. Caro,[1,2] and E. P. O'Reilly[1,2]
[1]*Tyndall National Institute, Lee Maltings, Cork, Ireland*
[2]*Department of Physics, University College Cork, Ireland*

(Received 28 April 2012; accepted 28 August 2012; published online 12 September 2012)

We present a detailed analysis of the electrostatic built-in field, the electronic structure, and the optical properties of *a*-plane GaN/AlN quantum dots with an arrowhead-shaped geometry. This geometry is based on extensive experimental analysis given in the literature. Our results indicate that the spatial overlap of electron and hole ground state wave functions is significantly increased, compared to that of a *c*-plane system, when taking the experimentally suggested trapezoid-shaped dot base into account. This finding is in agreement with experimental data on the optical properties of *a*-plane GaN/AlN quantum dots. © *2012 American Institute of Physics*. [http://dx.doi.org/10.1063/1.4752108]

The optical properties of conventional *c*-plane nitride-based heterostructures such as GaN/AlN quantum wells (QWs) or quantum dots (QDs) are limited by the strong electrostatic built-in fields arising in part from spontaneous and in part from strain-induced piezoelectric polarization effects.[1] Several different approaches have been discussed in the literature to reduce or even eliminate these built-in fields.[2–5] One of these approaches, which has been extensively studied in recent years, is the growth of nonpolar nitride-based QWs or QDs.[2,3] In these nonpolar systems, the *c*-plane lies within the growth plane. While in a nonpolar nitride-based QW the built-in field can be eliminated due to the absence of an interface along the *c*-axis, the built-in potential in a nonpolar QD is in principle very sensitive to the QD geometry and the resulting orientation of the facets along the *c*-axis.[6] Nevertheless, experimental studies revealed that in contrast to *c*-plane GaN/AlN QDs, their nonpolar *a*-plane counterparts exhibit no red-shift of the photoluminescence (PL) peak.[7] This feature indicates a strongly reduced electrostatic built-in field. Furthermore, the average PL lifetimes in *a*-plane GaN/AlN QDs have been found to be far shorter (one order of magnitude) than in *c*-plane dots, evidencing an increased spatial overlap of electron and hole wave functions due to the reduced built-in field.[3]

The electrostatic built-in field and its impact on the electronic and optical properties have been studied theoretically.[6,8,9] The properties of *a*-plane GaN/AlN QDs have been discussed in Ref. 6. The authors considered rectangular-based truncated pyramidal QDs, as suggested by initial experimental data,[10] and studied the built-in potential and the electronic structure as a function of the facet incline angle with respect to the *c*-plane. These theoretical investigations[6] indicated a strong reduction of the built-in potential in these nonpolar structures compared to their polar counterparts. However, both studies concluded that the spatial overlap of ground state electron and hole wave functions is significantly reduced in a nonpolar GaN/AlN QD compared to a realistic polar *c*-plane dot. This result originates mainly from the large spatial dimension, approximately 20 nm,[3,7,10] of the nonpolar GaN/AlN QD along the *c*-axis. This finding of reduced spatial overlap of electron and hole wave functions is in contradiction with the experimental data reported for example in Ref. 3. These previous theoretical studies, however, neglected the influence of the Coulomb interaction between the carriers. Recently, Schuh *et al.*[9] studied nonpolar InN/GaN QDs by means of an effective bond orbital model combined with configuration interaction (CI) calculations. This analysis revealed that, due to Coulomb effects, the excitonic ground states of polar and nonpolar InN/GaN QDs show about the same dipole strength.[9] Nevertheless, it should be noted that the assumed spatial extension of the studied nonpolar InN/GaN QD along the *c*-axis is 8 nm only. In conclusion, even when taking Coulomb interactions into account, the theoretical studies presented so far cannot fully explain the experimentally observed findings of a strong spatial overlap of electron and hole wave functions, and the resulting far shorter average PL lifetimes in nonpolar nitride-based QDs compared to their polar counterparts. Thus, the present theoretical study attempts to shed more light on the behavior of the built-in potential, the electronic structure, and the resulting optical properties of nonpolar GaN/AlN QDs.

Following the previous theoretical investigations, two key factors can be extracted as necessary for a realistic description of nonpolar nitride-based QDs. First, the QD geometry is of crucial importance since this significantly modifies the built-in field as well as the confinement potential for electrons and holes. Second, Coulomb effects have to be taken into account, since this contribution might compensate the spatial separation of electron and hole wave functions due to the presence of any built-in field. Founta *et al.*[11] performed very detailed experimental studies on the geometrical features of *a*-plane GaN/AlN QDs, indicating that these dots grow with a trapezoidal *arrowhead*-like base shape. Their geometrical features deviate significantly from the previously assumed truncated pyramidal or lens-shaped QD shapes.[6,8,9] To date no detailed analysis of the built-in field, the electronic, and the optical properties has been performed for arrowhead-shaped structures. Therefore, the aim of this work is to present a detailed analysis of realistic arrowhead-

 

shaped *a*-plane GaN/AlN QDs. We calculate the strain and the resulting built-in potential of the system under consideration in the framework of a continuum-based approach, including position dependent elastic constants, piezoelectric coefficients, and dielectric constants. Our strain field calculation is based on a staggered grid formalism,[12] and the associated built-in potential is obtained by solving Poisson's equation.[13] The electronic and optical properties are analyzed by means of a self-consistent Hartree calculation based on an effective mass approximation, taking different effective masses for electrons and holes along different directions into account. Our results show that the trapezoidal-shaped QD base, as indicated by the experimental findings in Ref. 11, changes the built-in potential significantly. As a result, the spatial overlap of electron and hole ground state wave functions in such an *a*-plane GaN/AlN QD increases significantly compared to that of a polar *c*-plane GaN/AlN QD. Our theoretical findings are therefore in agreement with the experimental observations of an increased spatial electron and hole wave function overlap due to the reduced built-in potential.[3,7]

Here, we focus our attention on *a*-plane GaN/AlN QDs for two reasons. First, we have shown that for nonpolar $In_xGa_{1-x}N$/GaN dots, with In contents of 5%-35%, the built-in field vanishes almost completely and one is left with a negligible potential difference between the QD facets along the *c*-axis.[8] Therefore, a high spatial overlap of electron and hole wave functions is expected. This prediction was recently confirmed by an experimental study[14] on nonpolar *m*-plane InGaN/GaN QDs. Second, in contrast to the InGaN system, detailed studies of the geometrical features of *a*-plane GaN/AlN QDs are given in the literature. As discussed above, knowledge of the QD geometry is of central importance for a realistic modeling of these structures. In Ref. 10 the atomic force microscopy (AFM) analysis of *a*-plane GaN/AlN QDs indicates that these structures form as truncated pyramids with average base size of 20 nm and heights of 2 nm. Similar dimensions have been found in Refs. 3 and 7. The study in Ref. 11 on the morphology of *a*-plane GaN/AlN QDs, which combined the use of complementary techniques [AFM, reflection high-energy electron diffraction, high-resolution transmission electron microscopy and scanning electron microscopy], revealed an even more precise picture of the dot geometry. A schematic illustration of the geometry deduced from these measurements is shown in Fig. 1. The experimental data[11] revealed (20-21)- and (02-21)-faces on two of the QD sides, which are at an angle of 33° with respect to the (11-20)-plane, while the other two faces lie in the (11-2-2)- and (11-21)-planes, at an angle of 32° and 17°, respectively, with the (11-20)-plane. The (02-21)- and the (20-21)-face are each at an angle $\alpha \approx 15°$ with respect to the *c*-axis. Therefore, following these experimental findings, we assume a truncated pyramidal QD structure with a height of 2 nm and a base length of $a = b = 20$ nm (cf. Fig. 1). The angles of the side facets are chosen according to Ref. 11. In addition, given that the incline angle $\alpha$, describing the angle between the *c*-axis and both the (20-21)- and (02-21)-plane, influences the *c*-plane oriented surface area, we also analyze how the magnitude of this angle influences the results.

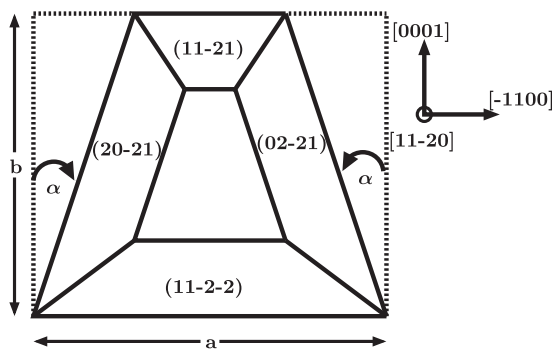


FIG. 1. Schematic view of a (11-20) nitride-based QD.

To study the optical properties of these nonpolar QD structures, knowledge of the single-particle states is required. We determine the single-particle states and energies by solving the Schrödinger equation:

$$H^\lambda \psi^\lambda(\mathbf{r}) = \left[-\frac{\hbar^2}{2}\nabla\frac{1}{m^\lambda(\mathbf{r})}\nabla + \tilde{V}^\lambda(\mathbf{r})\right]\psi^\lambda(\mathbf{r}) = E^\lambda\psi^\lambda(\mathbf{r}), \tag{1}$$

with $\tilde{V}^\lambda(\mathbf{r}) = V^\lambda(\mathbf{r}) + V_p(\mathbf{r})$. The bare confinement potential is given by $V^\lambda(\mathbf{r})$ while $V_p(\mathbf{r})$ denotes the built-in potential. The index $\lambda = e,h$ denotes electrons and holes, respectively. Additionally, for the electronic structure calculation of a QD, conduction band $\Delta E_c$ and valence band $\Delta E_v$ offset values are required, which enter Eq. (1) via $V^\lambda(\mathbf{r})$. Following our recent theory-experiment comparison on *a*-plane GaN/AlGaN QWs,[15] we use a conduction band to valence band offset ratio of $\Delta E_c : \Delta E_v \approx 45 : 55$. As in Ref. 15, we define the growth direction to be parallel to the *x*-direction. Neglecting the weak spin-orbit coupling, the three topmost valence bands (VBs) at $\mathbf{k} = \mathbf{0}$ can be classified as being $|X\rangle$-, $|Y\rangle$-, and $|Z\rangle$-like. The relative effective mass of the $|X\rangle$-like VB along the *x*-direction is approximately a factor of 10 smaller than for the $|Y\rangle$-like VB along this direction.[15] Consequently, the confinement along the *x*-direction leads to a large energetic separation of $|X\rangle$- and $|Y\rangle$-like VBs. The $|Z\rangle$-like VB is separated from the $|Y\rangle$-like VB due to the crystal field splitting, and shifted to lower energies with respect to the $|Y\rangle$-like VB. Therefore, the topmost VB at $\mathbf{k} = \mathbf{0}$ is predominantly $|Y\rangle$-like.[15] A more detailed discussion is given in Refs. 15 and 16. The material parameters are given in Ref. 15. Based on Refs. 15 and 16 and the fact that we are interested in the influence of the built-in field on electron and hole ground state wave functions only, an effective mass approximation should be sufficient to address this question.[17]

To analyze the influence of the Coulomb interaction on the results we apply a self-consistent Hartree approximation. Thus, the excitonic ground state is calculated using the ansatz of a separable exciton wave function $\psi_X(\mathbf{r}_e, \mathbf{r}_h) = \psi^e(\mathbf{r}_e)\psi^h(\mathbf{r}_h)$. The constituting electron $\psi^e(\mathbf{r}_e)$ and hole $\psi^h(\mathbf{r}_h)$ wave functions are determined self-consistently from

$$(H^e + V_h)\psi^e = \tilde{E}^e\psi^e, \quad (H^h + V_e)\psi^h = \tilde{E}^h\psi^h, \tag{2}$$

with

$$-e|\psi^e|^2 = \epsilon_0\nabla\cdot(\epsilon_r\nabla V_e)), \quad e|\psi^h|^2 = \epsilon_0\nabla\cdot(\epsilon_r\nabla V_h)).$$

Here, $H^{\lambda}$ is the single-particle Hamiltonian defined in Eq. (1). Therefore, the deformation of the single-particle wave functions under the influence of the Coulomb interaction is explicitly calculated, in order to minimize the total energy of the resulting many-body state. This approach is limited to the many-body ground state, since it requires only single-particle ground states. Schuh *et al.*[9] concluded for a pure InN/GaN dot that not only do the energetically lowest electron and hole single-particle states contribute to the many-body ground state but that higher states also do so. However, we find that for nonpolar arrowhead-shaped GaN/AlN QDs a self-consistent Hartree approximation is already sufficient to explain the experimental findings of an increased spatial overlap of electron and hole wave functions compared to that found in a polar dot. A more elaborate configuration interaction approach would therefore further support this result.

Having introduced the theoretical framework, we are now able to study how the built-in potential and consequently the spatial overlap of electron and hole ground state wave functions is changed when varying the QD geometry. In a first step we investigate the total (spontaneous + piezoelectric) built-in potential $\phi^{\text{tot}}$. Figure 2 shows $\phi^{\text{tot}}$ for a linescan along the $c$-axis, 0.8 nm above the QD base, as a function of $\alpha$, which is defined in Fig. 1. Due to the finite step size (0.4 nm) in the calculations, the curves show some ripples near the interfaces. The case $\alpha = 0°$ corresponds to a square-based truncated pyramidal QD, with inequivalent facets on the two (0001)-oriented faces. When looking at Fig. 2, one finds that $\phi^{\text{tot}}$ at the upper interface (in + $c$-direction) is significantly reduced when changing $\alpha$. This behavior originates from the fact that when increasing $\alpha$ the surface charge area will be reduced on the (11-21) dot face. Therefore, since both spontaneous and piezoelectric polarization depend on this area, both contributions will be reduced.[5] Thus, the potential difference between the top and the bottom QD interface along the $c$-axis will be reduced. Consequently, the spatial separation of electron and hole wave functions is reduced. Furthermore, inside and close to the upper interface, $\phi^{\text{tot}}$ becomes flat. As known from the $c$-plane QDs, the electron wave function is pushed to the upper interface due to $\phi^{\text{tot}}$. Thus, due to the flat built-in potential, the electron ground state wave function spreads considerably into the interior of the QD. Therefore, one expects with increasing $\alpha$ an increase of the spatial electron and hole wave function overlap.

For comparison, the line scan along the c-axis through the center of a truncated-cone shaped $c$-plane GaN QD is shown in Fig. 2. We assume a bottom diameter of 16 nm, a facet incline angle of 30° and a height of 3.2 nm. These dimensions are in agreement with experimental findings on $c$-plane dots.[19] In terms of $\phi^{\text{tot}}$, the experimentally observed[18] truncated pyramidal QDs with hexagonal base can be well approximated by a truncated cone.[16]

In the next step, we analyze the spatial overlap of electron $\psi^{e}_{\text{gs}}$ and hole $\psi^{h}_{\text{gs}}$ ground state wave functions, $d_{eh} = |\langle\psi^{e}_{\text{gs}}|\psi^{h}_{\text{gs}}\rangle|^2$, in arrowhead-shaped $a$-plane GaN QDs as a function of $\alpha$. Since experimental data[3] evidences an increased spatial electron and hole wave function overlap in $a$-plane GaN/AlN QDs compared to a $c$-plane structure, we have also evaluated $d_{eh}$ for a realistic $c$-plane GaN/AlN QD. The $c$-plane QD geometry and the dimensions are chosen as discussed above. For comparing the spatial overlap of $\psi^{e}_{\text{gs}}$ and $\psi^{h}_{\text{gs}}$ in $a$- and $c$-plane GaN/AlN QDs we study $\tilde{d}_{eh} = d^{a}_{eh}/d^{c}_{eh}$, where $d^{a}_{eh}$ denotes the overlap in the $a$-plane structure while $d^{c}_{eh}$ corresponds to the overlap in the $c$-plane dot. Figure 3 shows $\tilde{d}_{eh}$ as a function of $\alpha$. The experimentally suggested value $\alpha_{\text{exp}} \approx 15°$ is indicated by the dashed-dotted line. Additionally, $\psi^{e}_{\text{gs}}$ and $\psi^{h}_{\text{gs}}$ are shown in the $z$-$x$-plane (QD center), (a) without and (b) with Coulomb interaction. Focusing on the results based on a pure single-particle description (solid black line), Eq. (1), we observe that for $\alpha \leq 11°$ $\tilde{d}_{eh} < 1$ and therefore $d^{a}_{eh} < d^{c}_{eh}$. Nevertheless, with $\alpha > 11°$ $\tilde{d}_{eh} \geq 1$, even in a single-particle picture. In the presence of the Coulomb interaction (dashed red line), Eq. (2), $\tilde{d}_{eh} < 1$ ($d^{a}_{eh} < d^{c}_{eh}$) is observed for $\alpha < 6°$ only. From $\alpha > 6°$ $d^{a}_{eh}$ is significantly increased compared to $d^{c}_{eh}$, resulting in $\tilde{d}_{eh} > 1$. These findings are further supported by

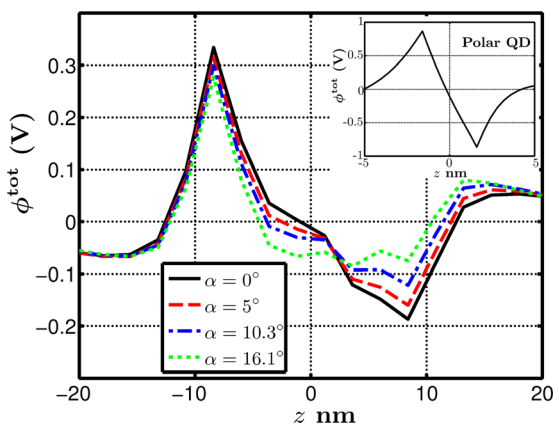


FIG. 2. Total (spontaneous+piezoelectric) built-in potential $\phi^{\text{tot}}$ for a linescan along the $z$-axis ($c$-axis) 0.8 nm above the QD base, as a function of $\alpha$ (cf., Fig. 1). Inset: Linescan through the polar GaN QD center along $c$-axis.

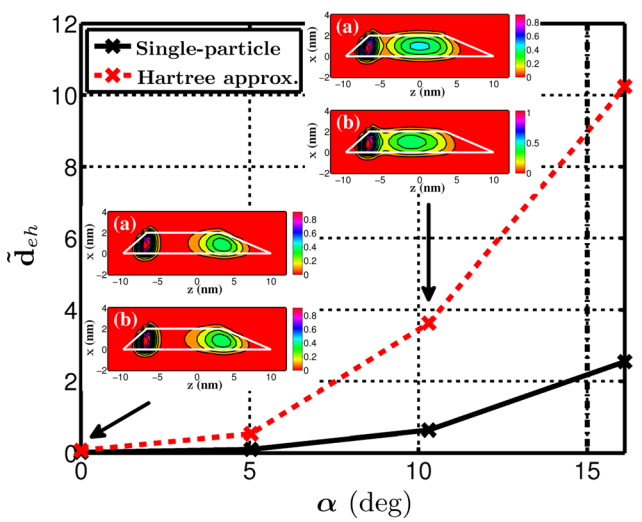


FIG. 3. Relative electron and hole wave function overlap $\tilde{d}_{eh}$ as a function of $\alpha$ for a nonpolar GaN QD with a base length $b = a = 20$ nm. The experimentally suggested value of $\alpha_{\text{exp}} = 15°$ is given by the dashed-dotted line. Results are shown without (solid line) and with (dashed line) Coulomb interaction. Insets show the electron and hole wave functions for a slice through the QD center (a) without and (b) with Coulomb interaction for $\alpha = 0°$ and $\alpha = 10.3°$.

the contour plots of $\psi^e_{gs}$ and $\psi^h_{gs}$ (cf. Fig. 3). When looking at $\alpha_{exp} = 15°$, we find that $d_{eh}$ for $\psi^e_{gs}$ and $\psi^h_{gs}$ in the *a*-plane GaN/AlN QD is increased by a factor of nine compared to the *c*-plane dot. Moreover, measurements on the radiative recombination time in *a*-plane GaN/AlN QDs give values which are one order of magnitude smaller than the ones obtained for *c*-plane QDs,[3] indicating a strongly increased spatial overlap of electron and hole wave functions. For $\alpha = 16°$, $\tilde{d}_{eh}$ is of order 10, tying in with the experiment.[3]

To further analyze the impact of the QD geometry on the results, we have also varied the size of the *a*-plane GaN/AlN QD. While keeping the *c*-plane dot unchanged, we have reduced the base lengths *a* and *b* of the *a*-plane structure from 20 nm to 16 nm. The main difference, compared to Fig. 3, is that $\tilde{d}_{eh}$ strongly increases. In this case even for the square-based nonpolar *a*-plane GaN/AlN dot $\tilde{d}_{eh} > 1$. Moreover, for $\alpha = 16°$, $\tilde{d}_{eh}$ is increased by a factor of almost eight compared to Fig. 3. This arises from two effects. First, due to the smaller average base length, the distance between the top and the bottom QD interface along the *c*-axis is decreased, leading already to a reduced potential drop across the structure and bringing $\psi^e_{gs}$ and $\psi^h_{gs}$ closer together. Second, the smaller base length reduces also the (0001)-oriented surface area and therefore the surface polarization charge density. Consequently, the built-in field is reduced compared to the system with a 20 nm base length. Again, this highlights the influence of the QD geometry on electronic and optical properties of *a*-plane GaN/AlN QDs. To further extend this analysis we have also compared $\tilde{d}_{eh}$ for an arrowhead-shaped QD with $\alpha = 10.3°$ to nonpolar GaN/AlN QDs with almost the same volume but a rectangular base. We find that the increase in $\tilde{d}_{eh}$, when going from a nonpolar square-based QD to an arrowhead-shaped QD, is not a pure volume effect. It is rather an interplay of volume effects, built-in field reduction, changes in the built-in potential profile inside the QD and changes in the quantum confinement for the carrier wave functions.

All of these findings emphasize that both the precise QD geometry and the Coulomb interaction between the charge carriers have to be taken into account for accurate modeling of the optical properties of *a*-plane GaN QDs.

In summary, we have investigated the influence of built-in fields on electronic and optical properties of realistic *a*-plane GaN/AlN QDs. The arrowhead-like structures considered are based on detailed experimental studies given in the literature.[11] Our analysis reveals that built-in fields, electronic, and optical properties are significantly modified by slight changes in the QD base geometry. More specifically, when deviating from a square- or rectangular-shaped QD base by assuming the experimentally indicated trapezoidal-shaped base the spatial overlap of electron and hole wave functions is strongly affected. Furthermore, comparing *a*-plane and realistic *c*-plane dots shows that when assuming the arrowhead-shaped structure the spatial electron and hole wave function overlap becomes considerably larger in the nonpolar system compared to the polar system considered. This increased spatial overlap in the nonpolar structure compared to the polar GaN/AlN QD system is in agreement with literature PL measurements on these two systems.[3]

This work has been supported by Science Foundation Ireland (Project Number 10/IN.1/I2994).

[1]C. J. Humphreys, MRS Bull. **33**, 459 (2008).
[2]P. Waltereit, O. Brandt, A. Trampert, H. T. Grahn, J. Menniger, M. Ramsteiner, and K. H. Ploog, Nature (London) **406**, 865 (2000).
[3]S. Founta, F. Rol, E. Bellet-Amalric, J. Bleuse, B. Daudin, B. Gayral, H. Mariette, and C. Moisson, Appl. Phys. Lett. **86**, 171901 (2005).
[4]K. C. Kim, M. C. Schmidt, H. Sato, F. Wu, N. Fellows, M. Saito, K. Fujito, J. S. Speck, S. Nakamura, and S. P. DenBaars, Phys. Stat. Sol. (RRL) **1**, 125 (2007); M. A. Caro, S. Schulz, S. B. Healy, and E. P. O'Reilly, J. Appl. Phys. **109**, 084110 (2011); M. Zhang, A. Banerjee, C.-S. Lee, J. M. Hinckley, and P. Bhattacharya, Appl. Phys. Lett. **98**, 221104 (2011).
[5]S. Schulz and E. P. O'Reilly, Phys. Rev. B **82**, 033411 (2010).
[6]S. Schulz, A. Berube, and E. P. O'Reilly, Phys. Rev. B **79**, 081401(R) (2009); O. Marquardt, T. Hickel, and J. Neugebauer, J. Appl. Phys. **106**, 083707 (2009).
[7]N. Garro, A. Cros, J. A. Budagosky, A. Cantarero, A. Vinattieri, M. Gurioli, S. Founta, H. Mariette, and B. Daudin, Appl. Phys. Lett. **87**, 011101 (2005).
[8]S. Schulz and E. P. O'Reilly, Phys. Stat. Sol. (c) **7**, 80 (2010).
[9]K. Schuh, S. Barthel, O. Marquardt, T. Hickel, J. Neugebauer, G. Czycholl, and F. Jahnke, Appl. Phys. Lett. **100**, 092103 (2012).
[10]S. Founta, F. Rol, E. Bellet-Amalric, E. Sarigiannidou, B. Gayral, C. Moisson, H. Mariette, and B. Daudin, Phys. Stat. Sol. (b) **243**, 3968 (2006).
[11]S. Founta, C. Bougerol, H. Mariette, B. Daudin, and P. Vennegues, J. Appl. Phys. **102**, 074304 (2007).
[12]K. S. Yee, IEEE Trans. Antennas Propag. **14**, 302 (1966).
[13]S. Schulz, M. A. Caro, E. P. O'Reilly, and O. Marquardt, Phys. Rev. B **84**, 125312 (2011).
[14]X. Yang, M. Arita, S. Kako, and Y. Arakawa, Appl. Phys. Lett. **99**, 061914 (2011).
[15]S. Schulz, T. J. Badcock, M. A. Moram, P. Dawson, M. J. Kappers, C. J. Humphreys, and E. P. O'Reilly, Phys. Rev. B **82**, 125318 (2010).
[16]D. P. Williams, S. Schulz, A. D. Andreev, and E. P. O'Reilly, J. Sel. Top. Quantum Electron. **15**, 1092 (2009).
[17]J. A. Barker and E. P. O'Reilly, Phys. Rev. B **61**, 13840 (2000).
[18]M. Arlery, J. L. Rouviere, F. Widmann, B. Daudin, G. Feuillet, and H. Mariette, Appl. Phys. Lett. **74**, 3287 (1999).
[19]F. Widmann, J. Simon, N. Pelekanos, B. Daudin, G. Feuillet, J. Rouvire, and G. Fishman, Microelectron. J. **30**, 353 (1999); M. Benaissa, P. Vennegues, and F. Semond, M. J. Condensed. Mater **11**, 43 (2009).